Zeolite Synthesis Hot Paper

Deutsche Ausgabe: DOI: 10.1002/ange.201501160
Internationale Ausgabe: DOI: 10.1002/anie.201501160

Widening Synthesis Bottlenecks: Realization of Ultrafast and Continuous-Flow Synthesis of High-Silica Zeolite SSZ-13 for NO_x Removal**

*Zhendong Liu, Toru Wakihara, Kazunori Oshima, Daisuke Nishioka, Yuusuke Hotta, Shanmugam P. Elangovan, Yutaka Yanaba, Takeshi Yoshikawa, Watcharop Chaikittisilp, Takeshi Matsuo, Takahiko Takewaki, and Tatsuya Okubo**

Abstract: *Characteristics of zeolite formation, such as being kinetically slow and thermodynamically metastable, are the main bottlenecks that obstruct a fast zeolite synthesis. We present an ultrafast route, the first of its kind, to synthesize high-silica zeolite SSZ-13 in 10 min, instead of the several days usually required. Fast heating in a tubular reactor helps avoid thermal lag, and the synergistic effect of addition of a SSZ-13 seed, choice of the proper aluminum source, and employment of high temperature prompted the crystallization. Thanks to the ultra-short period of synthesis, we established a continuous-flow preparation of SSZ-13. The fast-synthesized SSZ-13, after copper-ion exchange, exhibits outstanding performance in the ammonia selective catalytic reduction (NH_3-SCR) of nitrogen oxides (NO_x), showing it to be a superior catalyst for NO_x removal. Our results indicate that the formation of high-silica zeolites can be extremely fast if bottlenecks are effectively widened.*

Considerable effort is being made in emission control to meet the increasingly stringent legislative requirements.[1] Direct conversion of nitrogen oxides into N_2 and H_2O through ammonia selective catalytic reduction (NH_3-SCR) on metal-exchanged zeolites is the most promising technique for abating NO_x emission from diesel engines.[2] This prospect has motivated intensive studies on SSZ-13, a zeolite proven to be a superior candidate for use as a NH_3-SCR catalyst.[3] In addition to NO_x removal, SSZ-13 is also an excellent catalyst for the methanol-to-olefins reaction (MTO)[4] and direct conversion of ethylene into propylene (ETP).[5] However, synthesis of SSZ-13 takes a considerable time (typically more than 6 days).[6] Developing an efficient route to synthesize SSZ-13 is of high significance to meet the increasing demand for high-quality NH_3-SCR catalysts as well as to boost other applications of SSZ-13.

The slow kinetics of zeolite formation is a major obstacle to achieve efficient production.[7] In addition, zeolite is not the most thermodynamically stable phase but a metastable phase during the hydrothermal synthesis.[8] These features are especially pronounced for the synthesis of high-silica zeolites (Si/Al ratio larger than 6), primarily because the presence of negatively charged siloxy defects arising from insufficient aluminum tends to destabilize the zeolite framework or the nuclei required for zeolite formation.[9] Therefore, fast synthesis of high-silica zeolites is extremely challenging, since any single effort toward accelerating the crystallization rate may only result in the formation of co-crystallites or even a totally different phase.[10] A further problem is that the preparation of zeolites is usually conducted in a batch reactor. As this start-and-stop batch operation requires large space and huge investment, especially for larger scale productions, an alternative continuous-flow process, with pressure-tight and batch-free characteristics, could overcome such disadvantages.[11] The continuous-flow production of high-silica zeolites, if successful, would undoubtedly represent a milestone in zeolite science and technology. Hence, improving the crystallization kinetics and realizing ultrafast synthesis would be an essential step toward this goal.

Addressing the synthesis bottlenecks is the key in realizing ultrafast synthesis of high-silica zeolites. Herein, we demonstrate a comprehensive strategy, which considers both engineering and chemistry perspectives, to tackle the bottlenecks in sequence to develop an ultrafast synthesis of SSZ-13. First, from an engineering perspective, a tubular reactor was employed to avoid thermal time lag, which is a typical bottleneck in heat transfer in Teflon-lined autoclaves. Recently, we found that rapid heating in a tubular reactor combined with the addition of a zeolite seed allows the synthesis of aluminophosphate $AlPO_4$-5 (AFI topology) in 1 min.[12] Nevertheless, the crystallization mechanism of aluminosilicate differs from that of aluminophosphate.[13] In particular, the formation of SSZ-13 is kinetically much slower than that of $AlPO_4$-5. Therefore, more detailed considera-

[*] Z. Liu, Prof. Dr. T. Wakihara, Dr. S. P. Elangovan, Dr. W. Chaikittisilp, Prof. Dr. T. Okubo
Department of Chemical System Engineering
The University of Tokyo
7-3-1 Hongo, Bunkyo-ku, Tokyo 113-8656 (Japan)
E-mail: okubo@chemsys.t.u-tokyo.ac.jp
Dr. K. Oshima, D. Nishioka, Y. Hotta, T. Matsuo, T. Takewaki
Science and Technology Research Center
Mitsubishi Chemical Group
1000 Kamoshida-cho, Aoba-ku, Yokohama 227-8502 (Japan)
Y. Yanaba, Prof. Dr. T. Yoshikawa
Institute of Industrial Science, The University of Tokyo
4-6-1 Komaba, Meguro-ku, Tokyo, 153-8505 (Japan)

[**] This work is partially supported by Mitsubishi Chemical Corporation. T.O. is grateful to Grant-in-Aid for Scientific Research (A) Number 26249118 for financial support. Z.L. is grateful to the Ministry of Education, Culture, Sports, Science and Technology (Japan), for a Japanese Government Scholarship.

Supporting information for this article is available on the WWW under http://dx.doi.org/10.1002/anie.201501160.

tions from a chemistry perspective is needed to achieve ultrafast synthesis of SSZ-13. Our strategy aims at addressing the following issues: 1) reducing the synthesis period required for nucleation, 2) preventing the formation of undesired phase, and 3) breaking the equilibrium to enable a fast crystal growth. To this end, we found that the addition of a SSZ-13 seed bypasses the slow kinetics of spontaneous nucleation, a prime bottleneck in zeolite formation. Also, the seed plays a phase-determining role to ensure the formation of SSZ-13, a metastable phase in the synthesis. Further, the choice of effective starting materials together with the high temperature allows extremely fast crystal growth on the surface of the seed. The synergistic effect of these factors was found to be effective in easing the bottlenecks encountered in the overall crystallization process, resulting in a remarkable enhancement of crystallization.

With this strategy, we succeeded in achieving ultrafast synthesis of SSZ-13 within 10 min (Figure 1), a period remarkably shorter than several days reported in literature.[2b,3–6] The SEM image in Figure 1 b shows that the fast-synthesized SSZ-13 has a cubic shape with smooth facets, indicating high crystallinity. From solid-state ^{29}Si magic-angle spinning (MAS) NMR spectra (Figure 1 c), Si/Al ratios for the seed and the fast-synthesized SSZ-13 were calculated as 11.3 and 11.2, respectively. This result together with other characterizations (Figure S1, in the Supporting Information) confirms that the structural and textural characteristics of fast-synthesized SSZ-13 are the same as that of the SSZ-13 seed, which was synthesized using an autoclave.

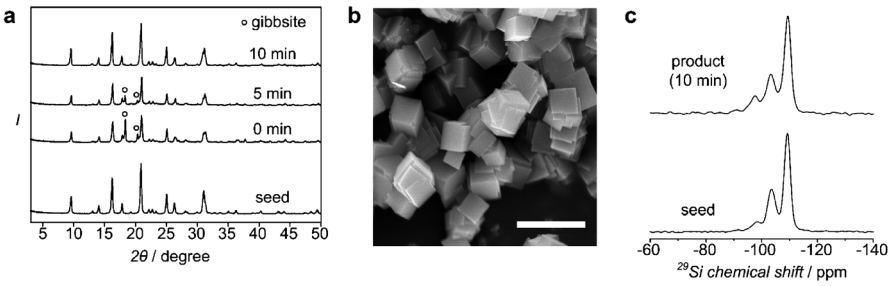

Figure 1. Ultrafast synthesis of zeolite SSZ-13 in 10 min. a) Powder X-ray diffraction patterns of the samples synthesized for 0 min, 5 min, and 10 min (the circles denote peaks arising from gibbsite, all other peaks are from SSZ-13) and for the SSZ-13 seed. b) SEM images of the SSZ-13 sample synthesized for 10 min (scale bar: 1 μm). c) Solid-state ^{29}Si MAS-NMR spectra for SSZ-13 seed and the product synthesized for 10 min.

Fast heating up in the tubular reactor is one of the factors essential to achieve the synthesis of SSZ-13 in 10 min. In contrast, even using the same gel with seed, it took 2 h to synthesize SSZ-13 in a conventional autoclave (Figure S2). The higher surface to volume ratio of the tubular reactor gives a much higher heating rate, making it efficient and avoiding the thermal lag.[12] Meanwhile, the tubular reactor, analogous to the continuous-flow reactor in shape, can also provide reliable kinetics data with high time resolution, which are required for designing a continuous-flow process.[14] It is worth noting that heating rate does not fundamentally change the crystallization rate of SSZ-13. To improve the slow kinetics, bottlenecks in nucleation and crystal growth should be tackled.

We chose to use a high temperature in our synthesis because it can significantly improve the crystallization rate. However, the synthesis at high temperature was possible only when the SSZ-13 seed was added. Under high temperature (210 °C), synthesis could complete in 10 min (Figure 1), whereas it took 8 h to synthesize SSZ-13 at 160 °C under otherwise similar conditions (Figure S3a). Clearly, a higher temperature dramatically accelerates the crystallization rate. The synthesis of SSZ-13 was normally conducted at moderate temperatures (130–165 °C), largely to avoid the formation of undesired phases.[3–6] In this sense, 210 °C would be overly high for the synthesis of SSZ-13. In fact, a different zeolite with MTN framework was obtained at 210 °C if no SSZ-13 seed was used (Figure 2). MTN has a higher framework density (18.7T/1000 Å) than that of SSZ-13 (CHA topology, 14.5T/1000 Å),[15] indicating that MTN is a more stable phase easily obtained at high temperatures. A comparison of syntheses with and without seed (Figure 1 and 2) clearly demonstrates that the SSZ-13 seed plays a crucial role in high-temperature synthesis. The seed serves as a phase-determining agent to ensure that the high-temperature synthesis produces pure phase of SSZ-13.

With an average particle size of 100 nm, the seed is very effective in avoiding spontaneous nucleation and thus greatly reduces the synthesis time. In the seed-assisted synthesis, an increase of crystallinity was observed once the gel was heated, whereas in the synthesis without seed, peaks arising from SSZ-13 can only be observed after a long-time synthesis of 3 days at 160 °C (Figure S3). The SSZ-13 seed does not apparently change during the fast synthesis, as demonstrated by the morphology evolution (Figure S4). Hence, crystallization of the newly formed SSZ-13 is considered to proceed directly on the surface of the seed.

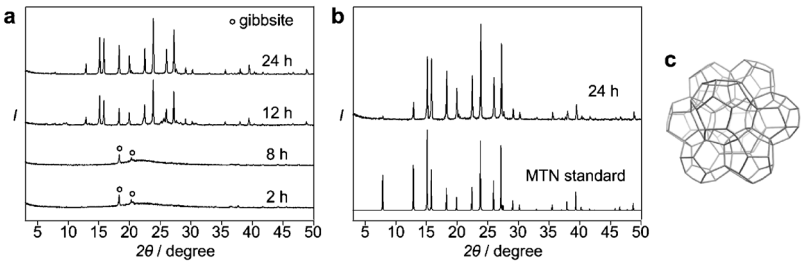

Figure 2. High-temperature synthesis without the addition of SSZ-13 seed (in autoclave). a) Powder X-ray diffraction patterns of the samples synthesized for different times (circles: gibbsite). b) Powder X-ray diffraction pattern for the sample synthesized for 24 h, referenced with standard pattern for MTN structure. c) illustration of MTN topology.

Compared to nucleation, crystal growth is usually considered a faster process.[2b] To achieve synthesis on the order of minutes, however, the bottleneck in the crystal growth step must be further eased. We identified that the choice of aluminum source was vital in reducing the energy barrier for fast crystal growth of SSZ-13 (Figure 3). Ultrafast synthesis of SSZ-13 could only be achieved when an aluminum hydroxide with the gibbsite structure (gibbsite $Al(OH)_3$) was used. In contrast, it took several hours to synthesize SSZ-13 for a non-crystalline aluminum hydroxide (non-crystalline $Al(OH)_3$; Figure S5). These results indicate that crystallization pathways vary with aluminum source. We found that the non-crystalline $Al(OH)_3$ tends to react with the colloidal silica to form a primary amorphous aluminosilicate, which is a relatively stable phase and thus not easy to convert into a crystalline product. On the contrary, with gibbsite $Al(OH)_3$ the reaction follows a pathway with lower energy barrier as it can avoid the generation of that primary amorphous aluminosilicate. From the solid-state ^{27}Al MAS NMR, a shift from $\delta = 0$ ppm to 55 ppm was observed for non-crystalline $Al(OH)_3$ once it was mixed with the colloidal silica (Figure 3d). Initially in an octahedral coordination environment, aluminum in the non-crystalline $Al(OH)_3$ immediately adopted a tetrahedral coordination environment, directly indicating the formation of the primary aluminosilicate network. In the case of gibbsite $Al(OH)_3$, however, the coordination environment of aluminum always remained octahedral until the completion of crystallization, indicating that release of aluminum is a gradual process concurrent with the progress of crystal growth (Figure 3e). Gibbsite $Al(OH)_3$ has a very low solubility ($K_{sp} = 3 \times 10^{-34}$ at 25 °C), which makes it unlikely to react with the colloidal silica to form that primary amorphous phase before the onset of crystallization. This phenomenon was also verified by the gradual disappearance of the gibbsite peaks in the X-ray diffraction (XRD) patterns (Figure 1a), SEM images (Figure S4), and the chemical composition of the solid products (Table S1) over different synthesis times.

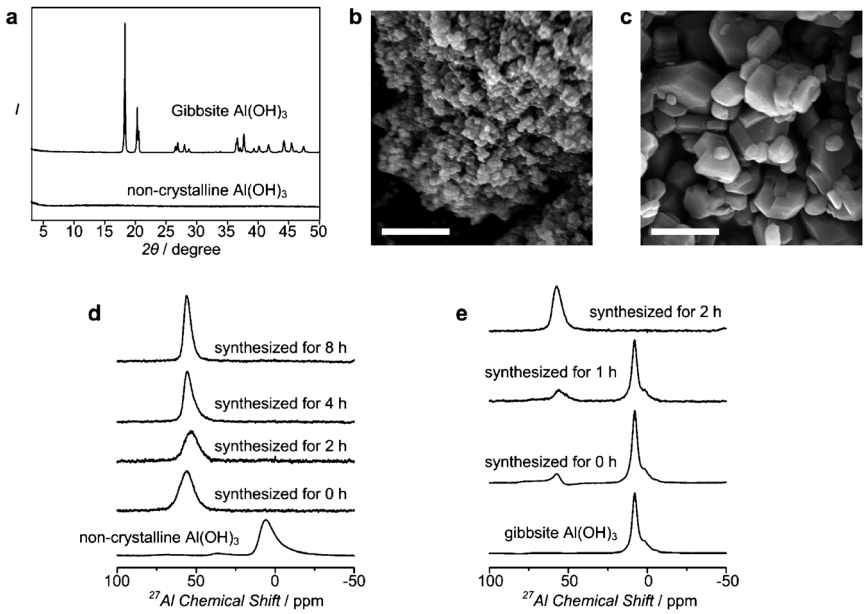

Figure 3. Syntheses using non-crystalline $Al(OH)_3$ and gibbsite $Al(OH)_3$ as aluminum sources. a) Powder X-ray diffraction patterns of the non-crystalline $Al(OH)_3$ and gibbsite $Al(OH)_3$. b) SEM photograph for the non-crystalline $Al(OH)_3$ (scale bar: 1 μm). c) SEM photograph for gibbsite $Al(OH)_3$ (scale bar: 1 μm). d) solid-state ^{27}Al MAS-NMR spectra for non-crystalline $Al(OH)_3$ and the samples synthesized over different periods using it as aluminum source. e) solid-state ^{27}Al MAS-NMR spectra for non-crystalline $Al(OH)_3$ and the samples synthesized over different periods using it as aluminum source. (Note that the syntheses were conducted in the autoclave, with seed and at 210 °C).

Though ultrafast synthesis on the order of minutes is an essential step, other factors need to be considered to realize a continuous-flow synthesis. The key to achieve continuous-flow preparation of high-silica zeolites is to match the kinetics, thermodynamics, and hydrodynamics (Figure 4a). Mismatch among these three factors may cause practical difficulties or even make continuous-flow synthesis impossible. In the

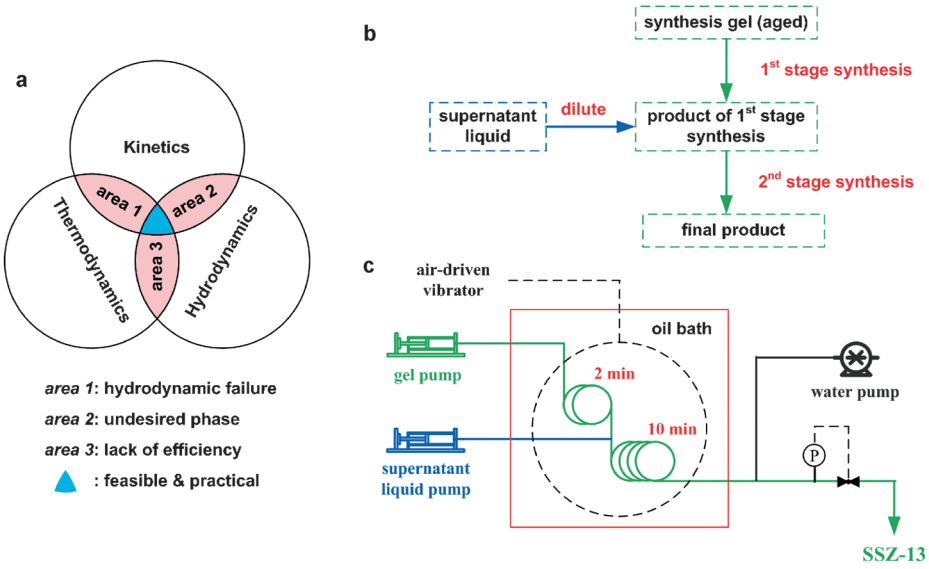

Figure 4. Continuous-flow preparation of zeolite SSZ-13. a) General guideline for developing a continuous-flow preparation of zeolites. b) Scheme of the procedure for two-stage synthesis. c) Flow chart for the continuous-flow preparation of SSZ-13.

synthesis of SSZ-13, we found that the gel viscosity sharply increased upon heating, causing gel fluidity to decline drastically (Figure S6). Thus, it would be impossible to keep an aluminosilicate gel with such high viscosity flowing for 10 min, which is the residence time required to get fully crystallized SSZ-13. One way to overcome this problem is to dilute the synthesis gel but not at the expense of a high crystallization rate. To this end, we developed a two-stage synthesis method in which the gel was diluted with a supernatant liquid in the middle of the process (Figure 4b). The introduction of the supernatant liquid significantly improved the fluidity of the gel. On the other hand, the use of the supernatant liquid did not alter the crystallization rate too much, largely because it provided a solution nearly in equilibrium with the final SSZ-13 crystals, as similarly discussed in previous work.[16] With a synthesis of 2 min (first stage) followed by an extra synthesis of 10 min after dilution with the supernatant liquid (second stage), fully crystallized SSZ-13 could be successfully obtained (Figure S7).

Based on this strategy, a two-stage continuous-flow system was designed to continuously synthesize SSZ-13 (Figure 4c). The residence times for the first and second stage were 2 and 10 min, respectively. An air-driven vibrator was used to improve the mixing of the supernatant liquid as well as to prevent precipitation inside the flow reactor. This design allowed a smooth continuous synthesis without any blockage problem (Figure S8). The product flowing out of the continuous-flow reactor proved to be fully crystallized SSZ-13 with the same properties as the sample prepared using the tubular reactor (Figure S9).

To explore the possibility of utilizing the fast-synthesized SSZ-13 as a NO_x removal catalyst, NH_3-SCR activity was tested on SSZ-13 seed and the fast-synthesized SSZ-13 (Figure 5). The samples were ion-exchanged to a similar level to make results comparable. As seen in Figure 5a, both fresh catalysts demonstrated similar catalytic results. Since the hydrothermal stability of zeolite is critical for its application as a NH_3-SCR catalyst, the catalytic performance was also measured after a hydrothermal treatment at 900 °C for 1 h. Similarly, both hydrothermally aged samples exhibited the same activity of NO_x reduction (Figure 5b). Note that SSZ-13 seed, similar to the one specifically developed for practical use as catalyst for NH_3-SCR and other applications,[2b,3–6] was synthesized in autoclave over several days. We therefore believe that the fast synthesized SSZ-13, with comparable catalytic performance, can be used as NO_x removal catalyst.

Although the synthesis of zeolites, a process initially achieved by mimicking the geological conditions of natural zeolites, had been believed to be slow, our results demonstrated that the crystal growth is not as slow as has been considered, provided the bottlenecks can be widened effectively. The strategy shown herein represents the most advanced technique to synthesize SSZ-13, and we anticipate that this method can be applied to other industrially important zeolites in the future.

Keywords: crystal growth · NO_x removal · heterogeneous catalysis · seeded growth · zeolites

How to cite: *Angew. Chem. Int. Ed.* **2015**, *54*, 5683–5687
Angew. Chem. **2015**, *127*, 5775–5779

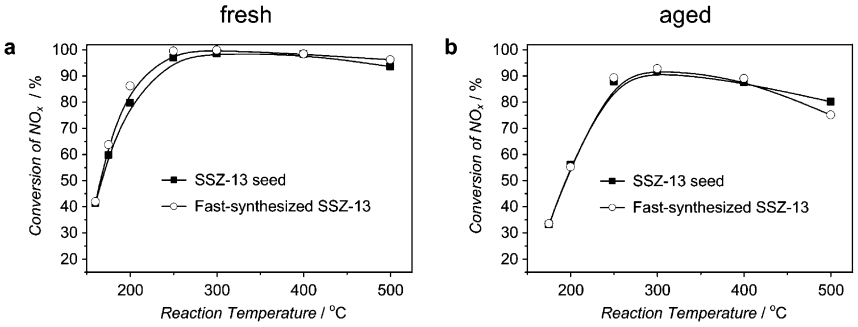

Figure 5. Conversion of NO_x in NH_3-SCR activity test. a) Conversion of NO_x for the fresh catalysts. b) Conversion of NO_x for the catalysts hydrothermally aged at 900 °C for 1 h.

[1] a) F. Thibault-Starzyk, E. Seguin, S. Thomas, M. Daturi, H. Arnolds, D. A. King, *Science* **2009**, *324*, 1048–1051; b) C. H. Kim, G. Qi, K. Dahlberg, W. Li, *Science* **2010**, *327*, 1624–1627.

[2] a) U. Deka, I. Lezcano-Gonzalez, B. M. Weckhuysen, A. M. Beale, *ACS Catal.* **2013**, *3*, 413–427; b) R. Martínez-Franco, M. Moliner, J. R. Thogersen, A. Corma, *ChemCatChem* **2013**, *5*, 3316–3323; c) M. Moliner, C. Franch, E. Palomares, M. Grill, A. Corma, *Chem. Commun.* **2012**, *48*, 8264–8266; d) C. H. F. Peden, J. H. Kwak, S. D. Burton, R. G. Tonkyn, D. H. Kim, J. H. Lee, H. W. Jen, G. G. Cavataio, Y. Cheng, C. K. Lambert, *Catal. Today* **2012**, *184*, 245–251; e) P. N. R. Vennestrøm, A. Katerinopoulou, R. R. Tiruvalam, A. Kustov, P. G. Moses, P. Concepcion, A. Corma, *ACS Catal.* **2013**, *3*, 2158–2161; f) A. Boubnov, H. W. P. Carvalho, D. E. Doronkin, T. Günter, E. Gallo, A. J. Atkins, C. R. Jacob, J. D. Grunwaldt, *J. Am. Chem. Soc.* **2014**, *136*, 13006–13015.

[3] a) F. Göltl, R. E. Bulo, J. Hafner, P. Sauter, *J. Phys. Chem. Lett.* **2013**, *4*, 2244–2249; b) F. Gao, J. H. Kwak, J. Szanyi, C. H. F. Peden, *Top. Catal.* **2013**, *56*, 1441–1459.

[4] a) Y. Bhawe, M. Moliner-Marin, J. D. Lunn, Y. Liu, A. Malek, M. Davis, *ACS Catal.* **2012**, *2*, 2490–2495; b) L. Wu, V. Degirmenci, P. C. Magusin, N. J. Lousberg, E. J. Hensen, *J. Catal.* **2013**, *298*, 27–40.

[5] Mitsubishi Chemical Corporation, Japanese Patent JP 2007–291076A, **2007**.

[6] a) S. I. Zones (Chevron Research Company), U.S. Patent 4,544,538, **1985**; b) S. I. Zones, R. A. Van Nordstrand, *Zeolites* **1988**, *8*, 166–174.

[7] a) M. E. Davis, *Nature* **2002**, *417*, 813–821; b) T. Wakihara, T. Okubo, *Chem. Lett.* **2005**, *34*, 276–281.

[8] a) E. P. Ng, D. Chateigner, T. Bein, V. Valtchev, S. Mintova, *Science* **2012**, *335*, 70–73; b) C. S. Cundy, P. A. Cox, *Microporous Mesoporous Mater.* **2005**, *82*, 1–78.

[9] A. W. Burton, S. I. Zones, S. Elomari, *Curr. Opin. Colloid Interface Sci.* **2005**, *10*, 211–219.

[10] V. Valtchev, A. Faust, J. Lézervant, *Microporous Mesoporous Mater.* **2004**, *68*, 91–95.

[11] a) C. Wiles, P. Watts, *Green Chem.* **2012**, *14*, 38–54; b) Z. Liu, Y. Lu, B. Yang, G. Luo, *Ind. Eng. Chem. Res.* **2011**, *50*,

11853 – 11862; c) G. S. Calabrese, S. Pissavini, *AIChE J.* **2011**, *57*, 828 – 834.
[12] Z. Liu, T. Wakihara, D. Nishioka, K. Oshima, T. Takewaki, T. Okubo, *Chem. Commun.* **2014**, *50*, 2526 – 2528.
[13] a) S. Oliver, A. Kuperman, A. Lough, G. A. Ozin, *Chem. Mater.* **1996**, *8*, 2391 – 2398; b) S. Oliver, A. Kuperman, A. Lough, G. A. Ozin, *Angew. Chem. Int. Ed.* **1998**, *37*, 46 – 62; *Angew. Chem.* **1998**, *110*, 48 – 64; c) J. Cejka, A. Corma, S. I. Zones, *Zeolites and Catalysis: synthesis, reaction and applications*, Wiley-VCH, Weinheim, **2010**.
[14] Z. Liu, T. Wakihara, D. Nishioka, K. Oshima, T. Takewaki, T. Okubo, *Chem. Mater.* **2014**, *26*, 2327 – 2331.
[15] J. L. Schlenker, F. G. Dwyer, E. E. Jenkins, W. J. Rohrbaugh, G. T. Kokotailo, *Nature* **1981**, *294*, 340 – 342.
[16] T. Wakihara, A. Ihara, S. Inagaki, J. Tatami, K. Sato, K. Komeya, T. Meguro, Y. Kubota, A. Nakahira, *Cryst. Growth Des.* **2011**, *11*, 5153 – 5158.

Received: February 6, 2015
Published online: March 20, 2015

